

Coherent Dynamical Recoupling of Diffusion-Driven Decoherence in Magnetic Resonance

Gonzalo A. Álvarez, Noam Shemesh, and Lucio Frydman*

Department of Chemical Physics, Weizmann Institute of Science, Rehovot, 76100, Israel

(Received 13 May 2013; published 20 August 2013)

During recent years, dynamical decoupling (DD) has gained relevance as a tool for manipulating and interrogating quantum systems. This is particularly relevant for spins involved in nuclear magnetic resonance (NMR), where DD sequences can be used to prolong quantum coherences, or to selectively couple or decouple the effects imposed by random environmental fluctuations. In this Letter, we show that these concepts can be exploited to selectively recouple diffusion processes in restricted spaces. The ensuing method provides a novel tool to measure restriction lengths in confined systems such as capillaries, pores or cells. The principles of this method for selectively recoupling diffusion-driven decoherence, its standing within the context of diffusion NMR, extensions to the characterization of other kinds of quantum fluctuations, and corroborating experiments, are presented.

DOI: [10.1103/PhysRevLett.111.080404](https://doi.org/10.1103/PhysRevLett.111.080404)

PACS numbers: 03.65.Yz, 76.60.Es, 76.60.Lz, 82.56.Lz

Introduction.—Understanding and manipulating the lifetimes of quantum coherences are central goals of contemporary physics. Quantum decoherence can be mitigated in several ways [1]; most often, this is achieved by rotation pulses that decouple the system from its environment. While such trains of refocusing pulses have been known since the early days of nuclear magnetic resonance (NMR) [2–4], these concepts have been generalized within the quantum information community by “dynamical decoupling” (DD) ideas [5–7]. These efforts aim at modulating the dephasing effects that environmental fluctuations impart on a quantum spin system, i.e., on filtering out modes in the environment’s spectral density noise. One form to achieve this entails designing DD sequences so that the time modulations experienced by the spins will minimize their overlap with the noise’s spectral density [6–9]. This is usually exploited to characterize an environment’s spectral density by varying the number of refocusing pulses or the interpulse delays [10,11]. Introducing such changes, however, may introduce complications of their own: varying the number of pulses may become a source of apparent decoherence via pulse imperfections [12]; and even if pulses are kept constant, varying their interpulse delay may lead to different total experimental times and hamper the measurement being sought, for instance, by imparting differing spin-spin relaxation (T_2) weightings. These complications can be avoided if DD sequences retain a constant overall duration and number of pulses [13,14], but depart from the dogma of using constant interpulse delays [7]. In NMR this has been suggested as a new magnetic resonance imaging (MRI) source of contrast [13]. In spectroscopic characterizations, the power of this concept was recently demonstrated by selective-dynamical-recoupling (SDR) sequences [14], where both the total evolution time and the number of pulses remain fixed, while the interpulse delay distribution is systematically varied. Unlike conventional

Carr-Purcell-Meiboom-Gill (CPMG) sequences [3], the SDR approach is immune to decoherence effects driven by cumulative pulse imperfections and/or to intrinsic T_2 spin-spin relaxation. SDR leads to a constant-time experiment with a fixed number of pulses, that can probe chemical identities via oscillatory modulations derived from chemical shifts [14].

This Letter addresses different kinds of decoherence effects, namely, those arising from spins diffusing in restricted spaces in the presence of a magnetic field gradient. Seeking improved ways of characterizing these phenomena has been a central theme in NMR and MRI [15,16], and has enabled a wide range of studies ranging from oil prospecting, to developmental brain studies—passing through many areas of physics, chemistry and biology [17,18]. As is shown here SDR can be a powerful approach to probe diffusion-related phenomena, while filtering pulse imperfections and intrinsic T_2 decay effects. This form of DD can probe the spectral density of a stochastic diffusion process, yielding information about the latter and reflecting in a straightforward manner the restricting lengths of the system. The ensuing approach turns out to be different from typical modulated gradient sequences in that, rather than probing a constant decay law that includes the diffusion spectrum [19–22], it probes how dynamics transition from free to restricted decay rates. This allows one to probe even very small ($\sim \mu\text{m}$) length scales, without requiring the very strong magnetic field gradients that are conventionally needed to observe diffusion-diffraction phenomena [15,23,24]. Furthermore, although this approach is illustrated here for NMR, it is a conceptually general way to probe noise correlation times—in particular those determining restricting length scales in complex systems.

To set the stage for this novel approach to monitor constrained diffusion, we first provide a general analysis of random translation under dynamical decoupling and its

relationship with spectral density. We then analyze the effects of free and restricted diffusion on the SDR modulations. Finally, we experimentally demonstrate how these modulations can be harnessed for accurately measuring compartment sizes under easily amenable conditions, in a noninvasive manner.

Modeling diffusion under dynamical decoupling.—Whereas the method proposed herein is general for probing fluctuations in a quantum two-level system interacting with a bath [4,6], we consider for conciseness an ensemble of $S = 1/2$ spins that do not interact with each other, but are coupled to a classical external magnetic field. This field involves a uniform component along the z axis defining a dominant Larmor frequency, and a perturbing linear field gradient G . Due to this gradient, diffusion-induced displacements will subject the spins to fluctuating precession frequencies. In a usual rotating frame of reference [4], the resulting Hamiltonian will be a pure dephasing system-environment (SE) interaction $\hat{\mathcal{H}}_{\text{SE}}(t) = \omega_{\text{SE}}(t)\hat{S}_z$, where $\omega_{\text{SE}}(t) = \gamma Gr(t)$ is the frequency (noise) felt by the spin, with r denoting the position of the diffusing spin along the field gradient direction $G = \partial B_z / \partial r$.

Consider the application of a sequence of strong π pulses as shown in Fig. 1(a), that periodically refocuses the spin ensemble after it has been subject to excitation. The sequence assumes N instantaneous pulses at times t_i , with an initial delay $t_1 - t_0 = x/2$ ($t_0 = 0$), uniform delays $t_i - t_{i-1} = x$ between the pulses for $i = 2, \dots, N-1$, and a final pulse at $t_N = \text{TE} - y/2$. $t_{N+1} = \text{TE}$ is the total evolution time (TE), and the x and y delays are such that $\text{TE} = y + (N-1)x$. Given the equidistant train of π pulses involved in the first part of the sequence we refer to it as involving a CPMG modulation [3], and to the final single-inversion part of the sequence as a Hahn modulation

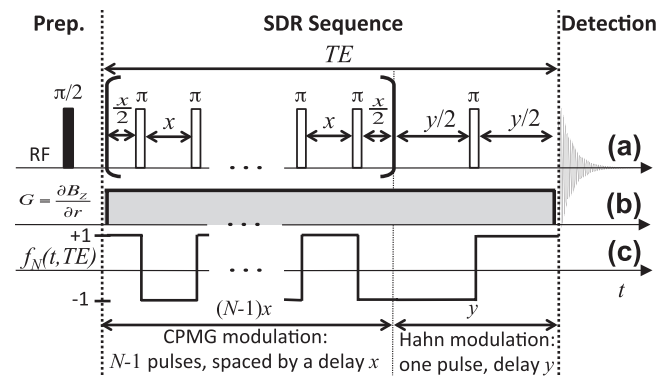


FIG. 1. Selective dynamical recoupling (SDR) sequence proposed for probing the diffusion spectrum, and involving (a) a sequence of N rf π pulses applied to the spins during a total evolution time TE; and (b) a constant magnetic field gradient G . A conventional CPMG sequence would arise if $x = y = \text{TE}/N$; we refer to the $N = 1$, $x = 0$ case as a Hahn-echo sequence. (c) Modulating function $f_N(t)$ imposed by the sequence of pulses.

[2]. This conforms to the SDR sequence [14] shown in Fig. 1. A constant gradient G given by an external action or local fields, is assumed to be active throughout the pulse train.

Under pulse-free conditions, the spin evolution operator for a given realization of a spatial random walk will be $\exp\{-i\phi(\text{TE})\hat{S}_z\}$, where $\phi(\text{TE})$ is the accumulated phase gained by the diffusing spin during TE. The effects that the pulse train in Fig. 1 will impose on the evolving spin can be accounted for by instantaneous sign changes of the evolution frequencies $\omega_{\text{SE}}(t)$. After applying the N pulses the accumulated phase will be $\phi(\text{TE}) = \int_0^{\text{TE}} dt' f_N(t', \text{TE}) \omega_{\text{SE}}(t')$, where the modulating function $f_N(t', \text{TE})$ switches between ± 1 as shown in Fig. 1(c). Given an initial state $\hat{\rho}_0 = \hat{S}_x$, the normalized magnetization arising from an ensemble of noninteracting and equivalent spins under the effects of this sequence will be $M(\text{TE}) = \langle e^{-i\phi(\text{TE})} \rangle$, where the brackets account for an ensemble average over the random phases. Without pulses $\langle \phi(\text{TE}) \rangle$ would depend on the position of each spin in the sample; as with all DD sequences, however, the average for the SDR case will be $\langle \phi(\text{TE}) \rangle = 0$. Thus, assuming that the random phase $\phi(t)$ has a Gaussian distribution [25,26], $M(\text{TE}) = \exp\{-(1/2)\langle \phi^2(\text{TE}) \rangle\}$: the signal will evidence a decay depending on the random phase's variance. This argument is solely given by the spins' diffusion within G , and can be written in a Fourier transform representation [6,20,21] as

$$\frac{1}{2} \langle \phi^2(\text{TE}) \rangle = \frac{\Delta \omega_{\text{SE}}^2}{2} \int_{-\infty}^{\infty} d\omega S(\omega) |F(\omega, \text{TE})|^2. \quad (1)$$

This expression entails a product of the spectral density $\Delta \omega_{\text{SE}}^2 S(\omega)$ characterizing the diffusion-driven fluctuation, times the filter function $F(\omega, \text{TE})$ given by the Fourier transform of the modulation function $\sqrt{2\pi} f_N(t', \text{TE})$. The spectral density $\Delta \omega_{\text{SE}}^2 S(\omega)$ is given in turn by the Fourier transform of the autocorrelation function $g(\tau) = \langle \Delta \omega_{\text{SE}}(t) \Delta \omega_{\text{SE}}(t + \tau) \rangle$, where $\Delta \omega_{\text{SE}}(t) = \gamma G[r(t) - \langle r(t) \rangle]$ is the spin's instantaneous frequency deviation from its average value, and $\Delta \omega_{\text{SE}}^2 = \langle \Delta \omega_{\text{SE}}^2(0) \rangle$. Assuming $g(\tau)$ follows an exponential decay, the spectral density of this fluctuation will be given by the Lorentzian function [25,27]

$$\frac{\mathcal{FT}\{g(\tau)\}}{\sqrt{2\pi}} = \Delta \omega_{\text{SE}}^2 S(\omega) = \frac{\Delta \omega_{\text{SE}}^2 \tau_c}{(1 + \omega^2 \tau_c^2) \pi}. \quad (2)$$

Here the correlation time τ_c will be associated to a characteristic length l_c , given by the diffusion process according to Einstein's expression $l_c^2 = 2D_0\tau_c$, where D_0 is the free diffusion coefficient. It also follows that $\Delta \omega_{\text{SE}}^2 = \gamma^2 G^2 D_0 \tau_c$. If considering now diffusion in a pore or restricted cavity, the specific relation between l_c and the restriction length d of the pore will depend on its geometry; e.g., for cylinders a good approximation is

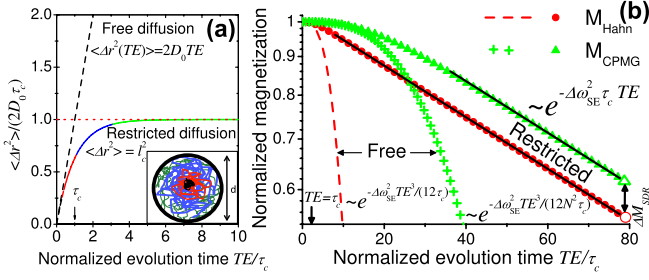


FIG. 2 (color online). (a) Normalized mean square displacement (solid multicolored line) of the diffusing spins in a restricted space. The dashed black line gives the free diffusion law while the dotted gives the restriction length l_c . The inset shows, in different colors, random trajectories for different total times within a cylinder of diameter d , where $l_c \approx 0.37d$. The same color tones are in the solid line to show the different time regimes of the spin trajectories. (b) Time evolution of the spin magnetization under CPMG ($N = 8$ pulses) and Hahn-echo sequences for spins diffusing in a restricted space (triangles, circles), and under free diffusion (crosses, dashes). The solid black lines show the time range where the restricted diffusion effects dominate; the difference ΔM_{SDR} between these lines gives a contrast, over which signals can be coherently modulated by a suitable SDR filter function.

$\tau_c \approx 0.26^2 d^2 / D_0$ [21,28] and then $l_c \approx 0.37d$, where d is the cylinder's diameter. Figure 2 compares the different behaviors that, in units of the correlation time τ_c , will be evidenced by the spin's mean displacement $\langle \Delta r(t)^2 \rangle = \langle [r(t) - r(0)]^2 \rangle$ depending on whether diffusion is free or restricted.

Restricted and free diffusion: Effects on the SDR modulations.—With this scenario as background, we consider the effects of the sequence in Fig. 1 for probing the behaviors illustrated in Fig. 2(a). The “gist” of SDR is that it manages to distinguish these cases without varying TE or the total number of intervening pulses, but rather using the flexibility that the delays x and y in Fig. 1 afford for shaping the $F(\omega, \text{TE})$ filter function. To see this more clearly, consider the two segments in the SDR sequence—the Hahn and the CPMG modulations—separately. The diffusion-driven signal decay for a Hahn-echo sequence [2] can be obtained analytically [29] (see the Supplemental Material [30]); its decay is shown in Fig. 2(b) by the red dashes and circles. Also the analytical expression for the signal decay of a CPMG sequence, characterized by N equispaced pulses ($x = y = \text{TE}/N$ in Fig. 1) can be calculated (see the Supplemental Material [30]); the ensuing magnetization decay is plotted in Fig. 2(b) (green crosses and triangles). The free diffusion regime exhibits the simplest behavior: since the delays between pulses $x, y \ll \tau_c$, the filter function F peaks at frequencies $\omega \gg 1/\tau_c$ [9,11] and decoherence effects are dominated by the tail of the spectral density $S(\omega) \propto (1/\omega^2 \tau_c \pi)$ [11,31]. The signal decay therefore follows a decay rate proportional to $\omega^{-2} = (\text{TE}/N)^2$ [dashes and crosses in Fig. 2(b)]. This result is

derived in the original CPMG paper for freely diffusing spins [3]. By contrast, in the restricted diffusion regime, τ_c is short due to the confinement. The delays between pulses $x, y \gg \tau_c$, and the dominant peaks of the filter functions F are at frequencies $\omega \ll 1/\tau_c$ [9,11]. In these cases the argument of the exponential function governing the signal decay will be

$$\frac{1}{2} \langle \phi^2(\text{TE}) \rangle \approx \Delta \omega_{\text{SE}}^2 \tau_c [\text{TE} - (1 + 2N)\tau_c]. \quad (3)$$

The exponential magnetization decay at a rate $\Delta \omega_{\text{SE}}^2 \tau_c$, is evidenced by the slopes in the solid black lines in Fig. 2(b). The second term in Eq. (3) [32] gives a shift depending on N , and is responsible for the ΔM_{SDR} gap separating the Hahn and the CPMG decays in Fig. 2(b). While normally the usual expression used for the restricted diffusion decay rate is just the first term of (3) [29], the second term derived here is unique to the SDR sequence and provides a new degree of freedom for probing restrictions according to the choice of x . In particular if $x \ll \tau_c \ll y$, the decay of the signal during the SDR is dominated by the Hahn portion of the sequence and approaches $M_{\text{Hahn}}^{\text{restricted}}(y) = \exp\{3\Delta \omega_{\text{SE}}^2 \tau_c^2\} \exp\{-\Delta \omega_{\text{SE}}^2 \tau_c y\}$, but if $x = y = \text{TE}/N \gg \tau_c$ the SDR decay will be $M_{\text{CPMG}}^{\text{restricted}}(\text{TE}, N) = \exp\{(1 + 2N)\Delta \omega_{\text{SE}}^2 \tau_c^2\} \exp\{-\Delta \omega_{\text{SE}}^2 \tau_c \text{TE}\}$. Thus, the SDR approach allows one to probe τ_c —and hence a confinement length l_c —from the difference between the Hahn and the CPMG decays (ΔM_{SDR}) that are built into the sequence. Notice that if $\text{TE}, y \gg \tau_c$,

$$\Delta M_{\text{SDR}} / M_{\text{Hahn}}^{\text{restricted}}(\text{TE}) = \exp\{2(N - 1)\Delta \omega_{\text{SE}}^2 \tau_c^2\} - 1$$

independently from TE, x or y . Moreover, while the exponential rate typically used for determining l_c is $\propto \Delta \omega_{\text{SE}}^2 \tau_c \propto l_c^4$, the shift term

$$\begin{aligned} \ln\{\Delta M_{\text{SDR}} / M_{\text{Hahn}}^{\text{restricted}}(\text{TE}) + 1\} &= 2(N - 1)\Delta \omega_{\text{SE}}^2 \tau_c^2 \\ &= (N - 1)l_c^6 \gamma^2 G^2 / (4D_0^2) \end{aligned}$$

amplifies this new source of contrast with N , and makes it a more sensitive reporter on the value of l_c as it is $\propto l_c^6$.

It follows that the sequence in Fig. 1 can interrogate restricted diffusion while fixing TE as well as the number of inversion pulses, by dividing an echo train into periods involving different interpulse delays x and y . By controlling the ratio x/y one can probe the spectral density $S(\omega)$ and determine the transition between Hahn- and CPMG-dominated regimes. The total sequence's time modulation f^{SDR} will then be given by

$$\begin{aligned} f_{N,x,y}^{\text{SDR}}(t, \text{TE}) &= f_{N-1}^{\text{CPMG}}(t, (N - 1)x) \\ &+ (-1)^{N-1} f_1^{\text{Hahn}}(t - (N - 1)x, y), \quad (4) \end{aligned}$$

where f_{N-1}^{CPMG} and f_1^{Hahn} are the CPMG and the Hahn modulating functions. The filter function $|F_{N,x,y}^{\text{SDR}}(\omega, \text{TE})|^2$ associated with SDR will thus be the sum of a CPMG

portion, a Hahn portion, plus a cross term representing an interference between these two filters:

$$|F_{N,x,y}^{\text{SDR}}(\omega, \text{TE})|^2 = |F_{N-1}^{\text{CPMG}}(\omega, (N-1)x)|^2 + |F_1^{\text{Hahn}}(\omega, y)|^2 \\ + (-1)^{N-1} 2 \text{Re}\{e^{i\omega(\text{TE}-y)} \\ \times F_{N-1}^{\text{CPMG}}(\omega, (N-1)x) \overline{F_1^{\text{Hahn}}(\omega, y)}\}. \quad (5)$$

This filter-function formalism allows one to derive a solution for the resulting signal decay

$$M_{\text{SDR}}(\text{TE}, x, y, N) = M_{\text{CPMG}}((N-1)x, N-1) M_{\text{Hahn}}(y) \\ \times M_{\text{Cross-SDR}}(\text{TE}, x, y, N), \quad (6)$$

whose analytical expression is given in the Supplemental Material [30]. It is worth concluding this paragraph by noting that the correlation time τ_c can also be extracted by comparing the exponential decay curves of independent Hahn and CPMG sequences, or by changing the N/TE ratio of a CPMG set. Such variations, however, would require comparing signal decays arising from measurements involving different number of pulses or different overall TE's. Only SDR manages to keep those parameters—whose variation could eclipse the diffusion effects being sought constant throughout the measurements.

SDR measurements of restriction lengths.—As proof of SDR's capabilities to accurately measure restricted diffusion, the sequence was applied to examine the diameter of water-filled microcapillaries with a nominal value of $5 \pm 1 \mu\text{m}$ (Polymicro Technologies, Phoenix, AZ, USA). A free diffusion coefficient $D_0 \sim 2.3 \times 10^{-5} \text{ cm}^2/\text{s}$ was measured by a conventional NMR sequence [23] in which the orientation of an applied gradient coincided with the principal axis of the microcapillaries. ^1H SDR curves of water diffusing within the capillaries were recorded in the presence of a transverse magnetic field gradient using a 9.4 T Bruker microimaging NMR scanner, where the effects of background gradients ($G = 0$) were found negligible. Figure 3 shows the SDR modulations observed as a function of x with $\text{TE} = 80 \text{ ms}$, for values of $G = 14.4$ and 21.6 G/cm . A transition from the diffusion-driven Hahn decay ($x \sim 0$) to the CPMG decay ($x = \text{TE}/N$) can be clearly appreciated in each data set; the difference between the $x = 0$ and $x = \text{TE}/N$ conditions, ΔM_{SDR} , together with the dependence on x in general, provide a robust determination of the diffusion's correlation time—and from there of l_c . The fit between the analytical expression derived for the SDR decay (Eqs. (S.5)–(S.22) in the Supplemental Material [30]) corresponding to particles diffusing in a cylinder [21,28] and the experimental data is excellent, and so is the agreement with the nominal inner diameter provided by the capillaries' supplier. Note the resemblance in the behavior of the SDR curves in Fig. 3 and the $\langle \Delta r^2 \rangle$ in Fig. 2(a): in both cases curves plateau for times $x > \tau_c$, evidence of a full sampling of the restricting space.

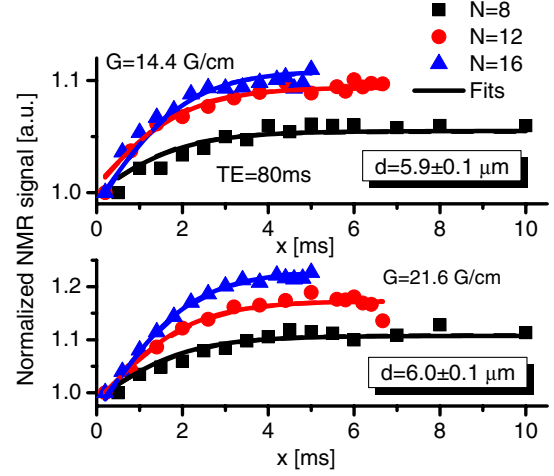


FIG. 3 (color online). Experimental SDR signals normalized with the first data point (symbols) as a function of the x delays. The solid lines are analytical fittings of Eq. (6) to the experimental curve. By using the measured diffusion coefficient $D_0 \sim 2.3 \times 10^{-5} \text{ cm}^2/\text{s}$, the fitted diameter d given in the plots is in agreement with the nominal value $d = 5 \pm 1 \mu\text{m}$.

Discussion.—The fact that the different ΔM_{SDR} measured by SDR at constant TE and N are solely defined by τ_c , provides a novel and simpler approach for determining restriction lengths l_c by NMR. Alternative noninvasive methodologies for probing the compartment dimensions, foremost among them diffusion-diffraction phenomena [15,23,24], require very strong magnetic field gradients—stronger by ~ 2 orders of magnitude than the gradients demanded by SDR, when small pores are considered. For example, measuring diffraction patterns in cylindrical pores characterized by a restricting length scale of $\sim 5 \mu\text{m}$ such as the ones used in this study, would require gradient amplitudes exceeding 1000 G/cm . Furthermore, methodologies that focus on probing a transition from free to restricted diffusion, will usually do so focusing on the deviations observed for the spectral density from power-law tails [19,21,22]. Instead, in the SDR case, the decay is dominated by the restricted diffusion regime: this makes ΔM_{SDR} a much more robust and sensitive means for determining length constraints. The resolvable restricting sizes of the ensuing method will eventually depend on the ratio $\Delta M_{\text{SDR}}/M_{\text{Hahn}}^{\text{restricted}}(\text{TE})$ being larger than the signal to noise ratio; among the factors that can magnify this ratio are N and G , which enhance ΔM_{SDR} as $(N-1)l_c^6 \gamma^2 G^2 / (4D_0^3)$. Probing restricted diffusion in tissues for example, where the diffusion coefficient $D_0 \sim 0.7 \times 10^{-5} \text{ cm}^2/\text{s}$, will lead to variations in $\Delta M_{\text{SDR}}/M_{\text{Hahn}}^{\text{restricted}}(\text{TE})$ of between 10%–250% for a compartment in the $1\text{--}1.5 \mu\text{m}$ range and typical gradient amplitudes of $\sim 50 \text{ G/cm}$ and $N = 16$. If stronger gradients ($> 500 \text{ G/cm}$) and spin-abundant porous systems are considered, sizes on the order of hundreds of nanometers should become clearly resolvable (depending on the intrinsic D_0 , which can also be

controlled via temperature). As N increases the sensitivity of the measurements also grows and the detectable size limits may be reduced even further. However, SDR's robustness will also depend on the accuracy of the refocusing pulses. Furthermore, SDR may be biased towards longer T_2 species, as a result of its constant-time nature.

This study demonstrated another instance where—as was the case with chemical exchange and J -coupling effects [14]—suitable DD schemes can extract coherent modulations from restricted NMR spectral fluctuations. As in previous spectroscopic demonstrations, a key ingredient to achieve these modulations is to have spins exchanging within a discrete or bound frequency spectrum, which DD can then probe by adjusting its filtering characteristics. The ensuing SDR method is particularly simple for determining the restricting length scales in complex, opaque systems [15,18] where the pore topology governs physical or biological properties of the materials. Applications of SDR to probe other kinds of constrained or pinned diffusive processes like charges diffusing in conducting crystals [33] or spin diffusion in molecules [34] can also be envisaged. Additionally, we expect that this method can be useful for imaging other kinds of spectra at the nanoscale; for example by sensing the correlation times of noise fluctuation generated by a host system on single spins in diamonds [35].

We are grateful to Pieter Smith, Guy Bensity, and Gershon Kurizki (Weizmann Institute) for fruitful discussions and to Prof. Yoram Cohen (Tel Aviv University) for providing the microcapillaries used in this study. This research was supported by a Helen and Martin Kimmel Award for Innovative Investigation, and the generosity of the Perlman Family Foundation. G. A. A. acknowledges the support of the European Commission under the Marie Curie Intra-European Fellowship for career Development Grant No. PIEF-GA-2012-328605.

*lucio.frydman@weizmann.ac.il

- [1] W. Zurek, *Rev. Mod. Phys.* **75**, 715 (2003).
- [2] E. Hahn, *Phys. Rev.* **80**, 580 (1950).
- [3] H. Carr and E. Purcell, *Phys. Rev.* **94**, 630 (1954); S. Meiboom and D. Gill, *Rev. Sci. Instrum.* **29**, 688 (1958).
- [4] A. Abragam, *Principles of Nuclear Magnetism* (Oxford University Press, London, 1961).
- [5] L. Viola, E. Knill, and S. Lloyd, *Phys. Rev. Lett.* **82**, 2417 (1999); K. Khodjasteh and D. A. Lidar, *ibid.* **95**, 180501 (2005).
- [6] A. G. Kofman and G. Kurizki, *Phys. Rev. Lett.* **87**, 270405 (2001).
- [7] G. S. Uhrig, *Phys. Rev. Lett.* **98**, 100504 (2007).
- [8] L. Cywinski, R. M. Lutchyn, C. P. Nave, and S. DasSarma, *Phys. Rev. B* **77**, 174509 (2008); G. Gordon, G. Kurizki, and D. A. Lidar, *Phys. Rev. Lett.* **101**, 010403 (2008); S. Pasini and G. S. Uhrig, *Phys. Rev. A* **81**, 012309 (2010).
- [9] A. Ajoy, G. A. Álvarez, and D. Suter, *Phys. Rev. A* **83**, 032303 (2011).
- [10] C. A. Meriles, L. Jiang, G. Goldstein, J. S. Hodges, J. Maze, M. D. Lukin, and P. Cappellaro, *J. Chem. Phys.* **133**, 124105 (2010); I. Almog, Y. Sagi, G. Gordon, G. Bensity, G. Kurizki, and N. Davidson, *J. Phys. B* **44**, 154006 (2011); J. Bylander, S. Gustavsson, F. Yan, F. Yoshihara, K. Harrabi, G. Fitch, D. G. Cory, Y. Nakamura, J. Tsai, and W. D. Oliver, *Nat. Phys.* **7**, 565 (2011).
- [11] G. A. Álvarez and D. Suter, *Phys. Rev. Lett.* **107**, 230501 (2011).
- [12] G. A. Álvarez, A. Ajoy, X. Peng, and D. Suter, *Phys. Rev. A* **82**, 042306 (2010); C. A. Ryan, J. S. Hodges, and D. G. Cory, *Phys. Rev. Lett.* **105**, 200402 (2010); A. M. Souza, G. A. Álvarez, and D. Suter, *ibid.* **106**, 240501 (2011); M. B. Franzoni, R. H. Acosta, H. M. Pastawski, and P. R. Levstein, *Phil. Trans. R. Soc. A* **370**, 4713 (2012).
- [13] E. R. Jenista, A. M. Stokes, R. T. Branca, and W. S. Warren, *J. Chem. Phys.* **131**, 204510 (2009).
- [14] P. E. S. Smith, G. Bensity, G. A. Alvarez, G. Kurizki, and L. Frydman, *Proc. Natl. Acad. Sci. U.S.A.* **109**, 5958 (2012).
- [15] P. Callaghan, A. Coy, D. MacGowan, K. Packer, and F. Zelaya, *Nature (London)* **351**, 467 (1991); P. T. Callaghan, *Translational Dynamics and Magnetic Resonance: Principles of Pulsed Gradient Spin Echo NMR* (Oxford University Press, New York, 2011).
- [16] W. S. Price, *Concepts Magn. Reson.* **9**, 299 (1997); P. N. Sen, *Concepts Magn. Reson.* **23A**, 1 (2004); D. S. Grebenkov, *Rev. Mod. Phys.* **79**, 1077 (2007).
- [17] P. Basser, J. Mattiello, and D. LeBihan, *Biophys. J.* **66**, 259 (1994); Y.-Q. Song, L. Zielinski, and S. Ryu, *Phys. Rev. Lett.* **100**, 248002 (2008).
- [18] V. Kukla, J. Kornatowski, D. Demuth, I. Girnus, H. Pfeifer, L. V. C. Rees, S. Schunk, K. K. Unger, and J. Kärger, *Science* **272**, 702 (1996); P. W. Kuchel, A. Coy, and P. Stilbs, *Magn. Reson. Med.* **37**, 637 (1997); S. Peled, D. G. Cory, S. A. Raymond, D. A. Kirschner, and F. A. Jolesz, *ibid.* **42**, 911 (1999); D. Le Bihan, *Nat. Rev. Neurosci.* **4**, 469 (2003); R. W. Mair, G. P. Wong, D. Hoffmann, M. D. Hürlimann, S. Patz, L. M. Schwartz, and R. L. Walsworth, *Phys. Rev. Lett.* **83**, 3324 (1999); Y.-Q. Song, S. Ryu, and P. N. Sen, *Nature (London)* **406**, 178 (2000).
- [19] P. P. Mitra, P. N. Sen, L. M. Schwartz, and P. Le Doussal, *Phys. Rev. Lett.* **68**, 3555 (1992).
- [20] P. T. Callaghan and J. Stepisnik, *J. Magn. Reson.* **117**, 118 (1995).
- [21] J. Stepisnik, S. Lasic, A. Mohoric, I. Sersa, and A. Sepe, *J. Magn. Reson.* **182**, 195 (2006).
- [22] J. C. Gore, J. Xu, D. C. Colvin, T. E. Yankeelov, E. C. Parsons, and M. D. Does, *NMR in Biomedicine* **23**, 745 (2010).
- [23] E. O. Stejskal and J. E. Tanner, *J. Chem. Phys.* **42**, 288 (1965).
- [24] N. Shemesh, C.-F. Westin, and Y. Cohen, *Phys. Rev. Lett.* **108**, 058103 (2012); F. B. Laun, T. A. Kuder, W. Semmler, and B. Stieltjes, *Phys. Rev. Lett.* **107**, 048102 (2011).
- [25] J. R. Klauder and P. W. Anderson, *Phys. Rev.* **125**, 912 (1962).
- [26] J. Stepisnik, *Physica (Amsterdam)* **270**, 110 (1999).

- [27] For a constant G and well defined cavity geometries, the spectral density is a sum of Lorentzians with different weights and correlations times [21,28]. However, usually one of them is more significant. At least for planar, spherical and cylindrical geometries, this dominant first term drives the SDR evolution.
- [28] J. Stepisnik, *Physica B (Amsterdam)* **183**, 343 (1993).
- [29] R.P. Kennan, J. Zhong, and J.C. Gore, *Magn. Reson. Med.* **31**, 9 (1994).
- [30] See Supplemental Material at <http://link.aps.org/supplemental/10.1103/PhysRevLett.111.080404> for the analytical expressions, their derivations, assumptions, and justifications.
- [31] D. Pfitsch, A. McDowell, and M.S. Conradi, *J. Magn. Reson.* **139**, 364 (1999).
- [32] Similar corrections to the decay argument only when $N = 0$ were obtained for Fermi golden rule decays in E.R. Fiori and H.M. Pastawski, *Chem. Phys. Lett.* **420**, 35 (2006).
- [33] A. Feintuch, A. Grayevsky, N. Kaplan, and E. Dormann, *Phys. Rev. Lett.* **92**, 156803 (2004).
- [34] N. Bloembergen, *Physica (Utrecht)* **15**, 386 (1949); D. Suter and R.R. Ernst, *Phys. Rev. B* **32**, 5608 (1985).
- [35] N. Zhao, J.-L. Hu, S.-W. Ho, J.T.K. Wan, and R.B. Liu, *Nat. Nanotechnol.* **6**, 242 (2011); T. Staudacher, F. Shi, S. Pezzagna, J. Meijer, J. Du, C.A. Meriles, F. Reinhard, and J. Wrachtrup, *Science* **339**, 561 (2013); S. Steinert, F. Ziem, L.T. Hall, A. Zappe, M. Schweikert, N. Götz, A. Aird, G. Balasubramanian, L. Hollenberg, and J. Wrachtrup, *Nat. Commun.* **4**, 1607 (2013).